Phys Chem Minerals (1995) 22:50–60

PHYSICS AND CHEMISTRY OF MINERALS

Thermally Induced Phase Transitions in Tridymite: an Infrared Spectroscopy Study

D. Cellai[1], **M.A. Carpenter**[1], **R.J. Kirkpatrick**[2], **E.K.H. Salje**[1], **M. Zhang**[1]

[1] Department of Earth Sciences, University of Cambridge, Downing Street, Cambridge CB2 3EQ, UK
[2] Department of Geology, University of Illinois, Urbana, Illinois 61801, USA

Received May 10, 1994 / Revised, accepted November 4, 1994

Abstract. The temperature dependence of the infrared active modes of meteoritic and synthetic tridymite have been investigated between 23 K and 1073 K in IR absorption and IR emission experiments. At room temperature both tridymite samples consist of a mixture of low temperature forms, in different proportions, due to the grinding. The sequence of phase transitions in Steinbach tridymite deduced from the IR data agrees well with recent X-ray and calorimetry studies using identical samples (Cellai et al. 1994). The previously suspected structural phase transition $P6_322 \Leftrightarrow P6_3/mmc$ is confirmed by the disappearance of the 470 cm^{-1} mode and a temperature anomaly of the spectral shift of the 790 cm^{-1} mode. Changes in the infrared spectra of synthetic tridymite give a different sequence of phase transitions from those of the meteoritic sample, consistent with the structural phase transitions observed in a ^{29}Si MAS NMR investigation using the same sample (Xiao et al. 1993).

Introduction

Heating from room temperature to 1000 K generates several displacive phase transitions in tridymite. These transitions have been studied by a variety of techniques, including optical microscopy with heating stages, single crystal or powder X-ray heating cameras, differential scanning calorimetry, infrared spectroscopy and nuclear magnetic resonance spectroscopy (complete references are given in recent papers by Smelik and Reeber 1990; Graetsch and Flörke 1991; De Dombal and Carpenter 1993; Xiao et al. 1993; Cellai et al. 1994). The complex series of transformations that occur during heating up to 523 K are not the same in samples of different origin (meteoritic, terrestrial, synthetic). Even in the same sample the thermal behaviour is strongly influenced by previous heat treatment and may not be reproducible, At higher temperatures, however, similar behaviour during the orthorhombic-hexagonal transition has been observed for different samples (as shown in the lattice parameters changes reported by Kihara 1978; Graetsch and Flörke 1991; De Dombal and Carpenter 1993; Cellai et al. 1994).

At room temperature three modifications of tridymite have been reported: monoclinic MC, pseudo-orthorhombic PO-*n* and monoclinic MX-1 (Table 1). Tridymite MC has a meteoritic or synthetic origin and its structure has been refined by Dollase and Baur (1976) and Kato and Nukui (1976). Terrestrial and some synthetic tridymites belong to the PO-*n* group (in the terminology of Nukui and Nakazawa 1980), in which *n* is the multiplicity of the *c* repeat relative to high temperature hexagonal tridymite. The structure of one terrestrial variant of this group with $n=10$ was refined by Konnert and Appleman (1978). MX-1 tridymite has an incommensurate structure and can be produced from MC crystals by grinding, in the preparation of powdered samples, or by quenching from 423 K to 273 K (Hoffmann et al. 1983).

Thermal behaviour of tridymite from the Steinbach meteorite has recently been examined by differential scanning calorimetry and X-ray diffraction using powders (De Dombal and Carpenter 1993) and single crystals (Cellai et al. 1994). Cellai et al. (1994) correlated the position of anomalous C_p effects with the phase transitions recognized by monitoring the change of a reflection violating the *c* glide. The sequence of phase transitions identified is reported in Fig. 1. Here we report the results of an infrared study of meteoritic and synthetic tridymite which leads to a more complete characterization of the phase transitions between room temperature and 1000 K.

Key features of what is already known about these phase transitions are:

(a) In the ideal high temperature structure of tridymite (phase HP, space group $P6_3/mmc$) the six fold rings of tetrahedra, which are oriented perpendicular to the *c* axis, are perfect hexagons. The Si–O–Si bond angles normal to the silica layers (Si–O1–Si) and those in

Correspondence to: D. Cellai

Table 1. Some crystallographic data for tridymite polymorphs

Phase	T (K)	Space group	Unit cell (Å)	Ref.
PO_{-n}	289	pseudo-orthorhombic	$a=17.22$ $b=9.93$ $c=nc_{hex}$	[a]
MX-1*	298	C1	$a=5.01$ $b=8.60$ $c=8.22$ $\beta=91.51$	[b]
MC**	298	*Cc*	$a=18.54$ $b=5.00$ $c=23.83$ $\beta=105.7$	[c]
OP	428	$P2_12_12_1$	$a=26.17$ $b=4.99$ $c=8.20$	[d]
OS	380–453	incommensurate superstructure	$a=105\text{-}65$	[e]
OS	423-463	metrically orthorhombic	$a=95\text{-}65$ $b=5.02$ $c=8.18$	[f]
OC	493	$C222_1$	$a=8.74$ $b=5.04$ $c=8.24$	[e]
LHP	673	$P6_322$	$a=5.05$ $c=8.27$	[g]
HP	733	$P6_3/mmc$	$a=5.05$ $c=8.27$	[h]

[a] Nukui and Nakazawa (1980); [e] Dollase (1967);
[b] Löns and Hoffmann (1987); [f] Nukui et al. (1978);
[c] Dollase and Baur (1976); [g] Cellai et al. (1994);
[d] Kihara (1977); [h] Kihara (1978)

* Phase with incommensurate modulation
** Hoffman (1967) setting ist: $a=18.5$ Å; $b=5.0$ Å; $c=25.8$ Å; $\beta=118°$

the layer (Si–O2–Si) are 180°, as imposed by symmetry. However, structure refinements of the HP phase (Kihara 1978; Kihara et al. 1986) revealed that both these oxygens have unusually large and anisotropic thermal parameters, indicating strong positional disorder. The directions of the largest thermal vibrational components of O1 (apical oxygen) and O2 (basal oxygen) are perpendicular to the Si–Si axis, i.e. perpendicular and parallel to the c-axis respectively. The O1 and O2 atoms undergo coupled thermal vibrations in order to minimize the repulsion between the O atoms and keep the Si–O bond distance constant. Kihara and coworkers treated the residual densities observed in difference Fourier maps as six fold oxygen split positions, in which the oxygen occupies, statistically, all six positions on the circumference of a circle of radius 0.4 Å perpendicular to the Si–Si axis. In this model the tridymite does not have the ideal structure proposed by Gibbs (1927) but has tilted tetrahedra with a mean Si–O–Si bond angle of 149.2°. The average position of the oxygen still gives an apparent Si–O–Si bond angle of 180° and this preserves the $P6_3/mmc$ symmetry. The form of the density contours around the atomic positions (average position) does not, however, show whether the oxygens are located in discrete positions around a space-averaged mean position (static disorder), or whether they can vibrate thermally about a time – averaged mean position (dynamic disorder).

(b) As the temperature decreases below the stability field of the HP phase down to 383 K a complex sequence of phase transitions occurs, involving oxygen disorder. The disorder of O is reduced significantly only at 383 K when the structure collapses into the monoclinic MC phase (Kihara 1978; Kihara et al. 1986).

(c) Two different sequences of transformations occur for single crystals of MC tridymite on heating from room

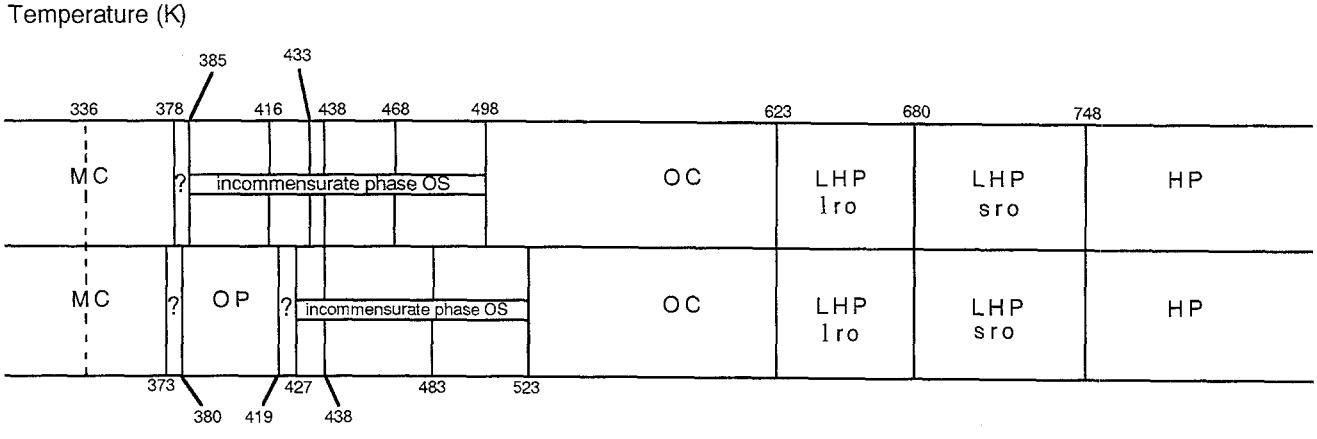

Fig. 1. Thermal changes of Steinbach tridymite as determined from Cp anomalies and changes in the intensity of a reflection violating the c glide (Cellai et al. 1994). The transition at 623 K has been determined by De Dombal and Carpenter (1993) by measuring the lattice parameters. Unannealed sample (*upper*) and sample annealed in the stability field of the hexagonal phase (*lower*). The main difference between these two transformation sequences is the presence of the OP phase in the annealed sample. Differences in transition temperatures between these two starting sample also occur. Transition temperatures within the OS phase correspond to Cp anomalies, which may reflect changes of the satellite reflections of the OS phase. Iro refers to long range order and sro to short range order in the LHP phase. *Dashed line* indicates the MX-1 transition which occurs when the MC crystals of tridymite are ground into a powder so that the MX-1 phase is formed. This transition temperature varies from crystal to crystal and 336 K represent the maximum of the distribution curve of the transition temperatures of 200 crystals (Hoffmann et al. 1983)

temperature to 523 K. According to Nukui et al. (1978) synthetic tridymite transforms at 383 K into the orthorhombic OP phase (space group $P2_12_12_1$), at 433 K to the incommensurate OS phase, and then at about 463 K to the orthorhombic OC phase (space group $C222_1$). Cellai et al. (1994) have pointed out that the OP phase appears in the meteoritic tridymite only if the sample has been previously annealed at high temperatures (in the stability field of the hexagonal phase). For unannealed samples the sequence of transformations is different, and appears to be MC⇔OS⇔OC. This difference is shown in Fig. 1.

(d) When single crystals of MC tridymite are ground into a powder or are quenched to 283 K from a temperature between 383 K and 433 K the phase MX-1 is formed. According to the X-ray precession photographs of Hoffmann et al. (1983) this phase transforms to PO phase on heating. The transition temperature differs from crystal to crystal but is in the temperature range 308 K to 353 K. The PO phase then displays the same transition behaviour as MC tridymite (Nukui and Nakazawa 1980).

(d) There is some controversy with respect to the temperature of the OS⇔OC transition; transition temperatures between 453 K and 523 K have been reported, but might change depending on the starting material and the thermal heating and cooling cycles employed.

(e) Cellai et al. (1994), on the basis of differential scanning calorimetry and X-ray diffraction data, have reported a second order transition at 680 K between two hexagonal phases (Fig. 1). This transition is believed to be due to the symmetry change $P6_322$ (LHP) ⇔ $P6_3/mmc$ (HP) and involves the loss of the centre of symmetry.

Crystallographic data for tridymite polymorphs are reported in Table 1. Results of factor group analysis for HP, LHP, OC and MC are given in Table 2.

Table 2. Vibrational modes in hexagonal, orthorhombic and monoclinic tridymite

$P6_3/mmc$	(HP)	Total irreducible representation $\Gamma = A_{1g}+2B_{1g}+E_{1g}+2E_{2g}+A_{1u}+4A_{2u}$ $+B_{1u}+3B_{2u}+5E_{1u}+4E_{2u}$ Accoustic modes $\Gamma_{ac} = A_{2u}+E_{1u}$ Optically active modes $\Gamma_{opt} = A_{1g}+E_{1g}+2E_{2g}$ (Raman active) $+3A_{2u}+4E_{1u}$ (Infrared active)
$P6_322$	(LHP)	Total irreducible representation $\Gamma = 2A_1+4A_2+3B_1+3B_2+6E_1+6E_2$ Acoustic modes $\Gamma_{ac} = A_2+E_1$ Optically active modes $\Gamma_{opt} = 2A_1+6E_2$ (Raman active) $+3A_2$ (Infrared active) $+5E_1$ (Raman and Infrared active)
$C222_1$	(OC)	Total irreducible representation $\Gamma = 8A+10B_1+9B_2+9B_3$ Acoustic modes $\Gamma_{ac} = B_1+B_2+B_3$ Optically active modes $\Gamma_{opt} = 8A$ (Raman active) $+9B_1+8B_2+8B_3$ (Raman and Infrared active)
Cc	(MC)	Total irreducible representation $\Gamma = 108A'+108''$ Acoustic modes $\Gamma_{ac} = 2A'+1A''$ Optically active modes $\Gamma_{opt} = 106A'+107A''$ (Raman and Infrared active)

Sample Description and Experimental Methods

We have investigated two samples: a natural and a synthetic tridymite. The natural sample, from Steinbach meteorite, was provided by the British Natural History Museum (no. 33450), Steinbach tridymite is monoclinic (phase MC) at room temperature and its structure has been determined by Dollase and Baur (1976). The synthetic tridymite was grown from Na_2WO_4 flux doped with 0.1% $FeCl_3$. TEM and X-ray diffraction shown that the symmetry is monoclinic (phase MC). The sample of this synthetic tridymite has been described by Xiao et al. (1993). For infrared measurements the samples were ground for about 1 minute into a powder by hand using a mortar and pestle. In order to examine the effect of grinding as small amount of each sample was also milled using a Spex-Mill. For IR absorption experiments the standard pellet technique was used by diluting tridymite powder in KBr (for mid infrared) or CsI (for far infrared) in the ratio 1:350 for natural tridymite and 1:50 for the synthetic tridymite. For some samples this ratio needed to be increased to 1:1500 or 1:750, as the strongest peaks were saturated in the spectra. For emission infrared spectroscopy only 0.15 mg of hand ground sample was used.

The infrared spectra were collected under vacuum using a Fourier transformation infrared spectroscopy (Bruker IFS 113v). The sample was positioned in a cylindrical platinum-wound furnace in the sample compartment. The sample temperature was measured using a Pt−Rh thermocouple held in contact with the sample. The sample temperature was controlled using a Eurotherm temperature control system to a stability of ±1 K. Spectra have been measured at low temperatures using a Leybold closed-cycle liquid helium refrigeration, in order to reduce the thermal line broadening. The spectral resolution was set to 2 cm^{-1} for middle infrared, to 4 cm^{-1} for far infrared and to 6 cm^{-1} for emission spectra. The zero filling factor for the Fourier transform algorithm was 4, hence a final spectral resolution of 0.5 cm^{-1}, 1 cm^{-1}, 1.5 cm^{-1} respectively were obtained. Spectra were analysed by least-squares fitting of Lorentzian peak profiles using the program "Razor". The positions, widths and heights of the peaks, as well as the baseline, were refined simultaneously, The error involved in the fitting was ±0.2 cm^{-1} for the peak positions, and the maximum error for the integrated intensities was ±20%.

Three IR absorption experiments were performed on three different Steinbach samples in the region 250–680 cm^{-1}: a heating run, from room temperature to 693 K using a hand ground sample, and cooling runs from room temperature to 23 K using hand ground and milled samples. One emission experiment was performed from 423 K to 1073 K in the region 600–1400 cm^{-1} using hand ground Steinbach tridymite. Three IR absorption experiments were performed on three different synthetic samples: two heating runs from room temperature to 340 K in the region 519–1500 cm^{-1} for milled samples, and in the region 520–900 cm^{-1} for hand-ground tridymite. In the same region (520–900 cm^{-1}) the cooling run from room temperature to 23 K was performed using a milled sample.

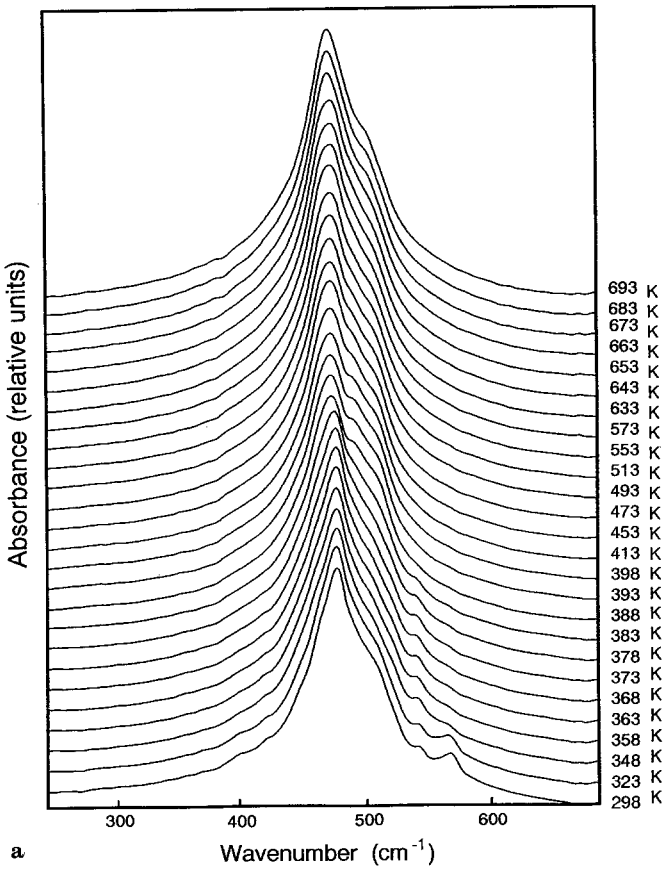

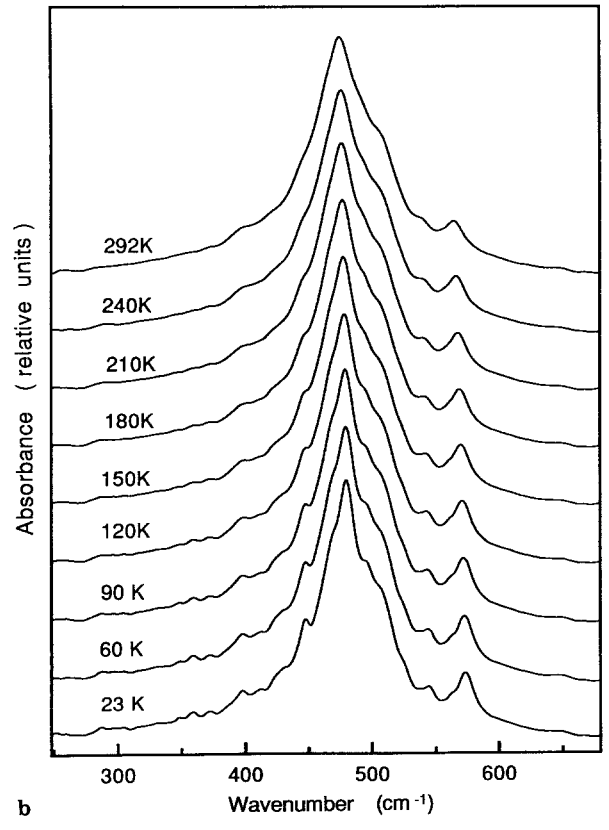

Fig. 2a, b. IR absorption spectra of hand-ground Steinbach tridymite (**a**) from room temperature to 693 K and (**b**) from room temperature to 23 K

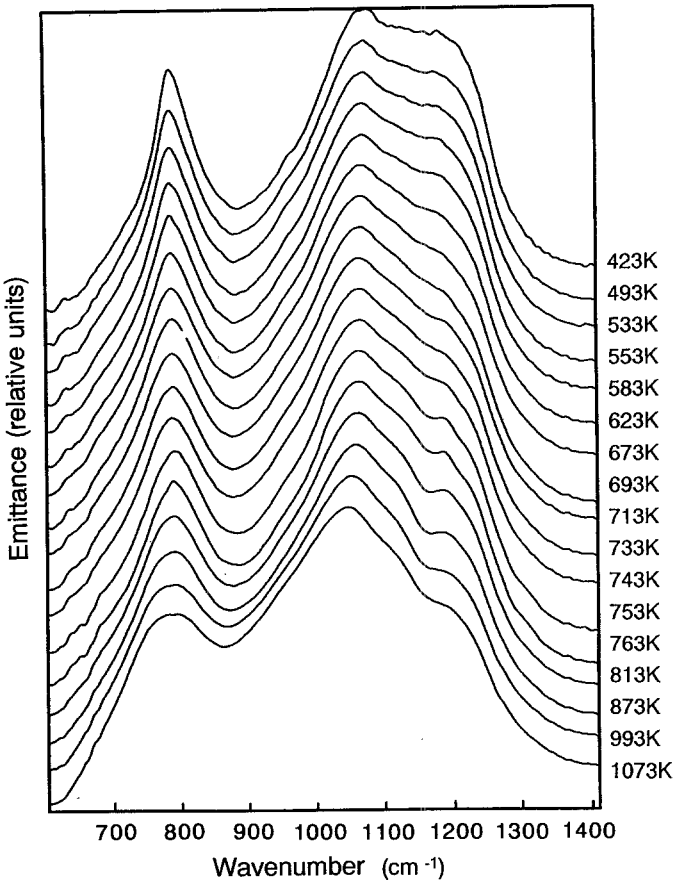

Fig. 3. Selected emission spectra of hand-ground Steinbach tridymite from 423 K to 1073 K

Results

Steinbach Tridymite

The spectra of Steinbach tridymite, for the spectral range from 250 cm^{-1} to 680 cm^{-1} and from 600 cm^{-1} to 1400 cm^{-1} are shown in Fig. 2 and Fig. 3, respectively. The spectra are broadly similar to those of quartz, with well separated stretching modes between 900 cm^{-1} and 1400 cm^{-1}, and bending modes near 780 cm^{-1} as well as between 400 cm^{-1} and 600 cm^{-1}. A general assignment can be taken from the well known behaviour of quartz.

Closer inspection of the phonon bands near 480 cm^{-1} (Fig. 2) shows only two phonons at 460 cm^{-1} and 490 cm^{-1} in this spectral region for the HP phase, in accordance with group theoretical predictions. Lowering the temperature splits these phonon branches, and we find at room temperature about 11 different phonon signals. Although some modes show weak absorption, they are important for this study because these signals are characteristic of specific phases of tridymite. Following the temperature evolution of this band to lower temperatures we find a further splitting of phonon lines at 23 K, together with newly emerging signals between 250 cm^{-1} and 380 cm^{-1} (Fig. 2b). The intensities of these signals are weak because their physical origin lies in the increase

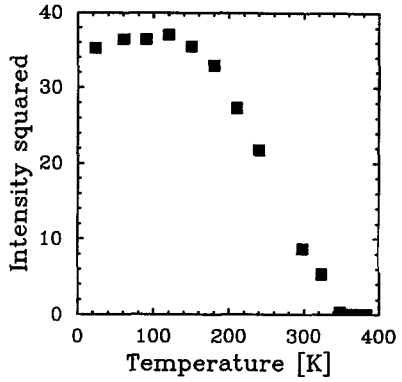

Fig. 4. Temperature dependence of the square of the integrated intensity of the 570 cm^{-1} mode for hand ground Steinbach tridymite. The intensity correlates with the temperature, except in the saturation regime below 200 K

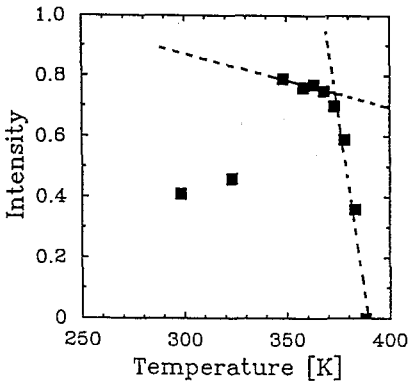

Fig. 6. Temperature evolution of the integrated intensity (arbritary units) of the 540 cm^{-1} mode for hand-ground Steinbach tridymite. This mode disappears at 388 K and two discontinuities at 348 K and 373 K can clearly be seen. *Dashed lines* are a guide for the eye to emphasize the breaks in slope

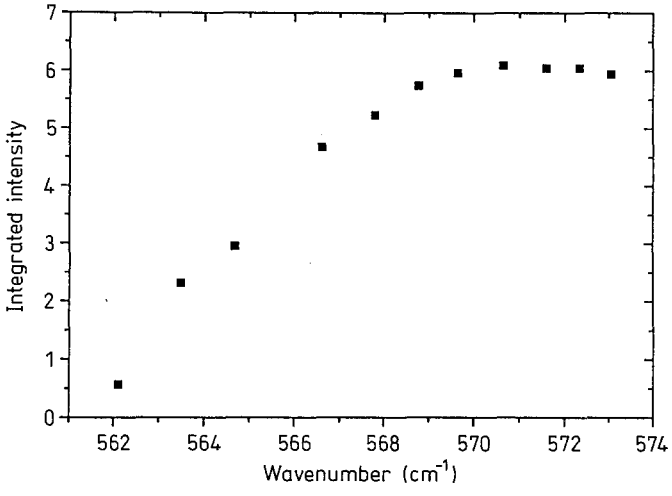

Fig. 5. Frequency dependence of the integrated intensity (arbitrary units) of the 570 cm^{-1} mode for hand-ground Steinbach tridymite showing a correlation except in the saturation regime (below 569 cm^{-1})

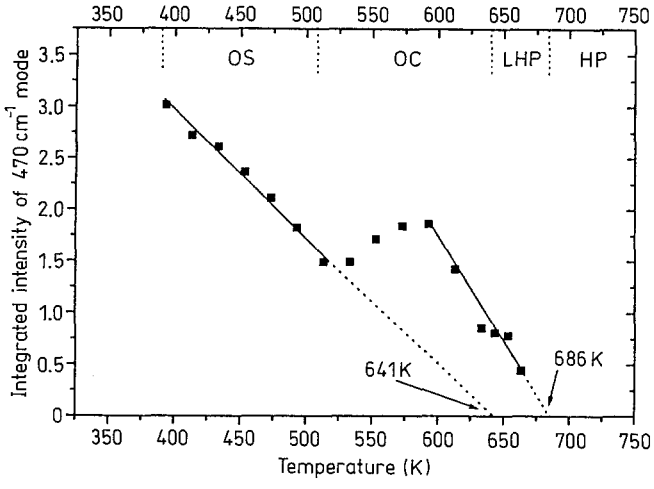

Fig. 7. Temperature dependence of the integrated intensity (arbitrary units) of the 470 cm^{-1} mode for hand-ground Steinbach tridymite. The band shows transition-related changes (see text)

of the unit cell dimension and the equivalent backfolding of phonon branches which were situated at the surface of the Brillouin zone at higher temperatures. The influence of structural phase transitions is seen as subtle changes of virtually all modes.

Let us now focus on the phonon near 570 cm^{-1} as an example. This mode disappears at ~348 K (Fig. 4) and coincides with the MX-1⇔PO transition reported by Hoffmann et al. (1983). Its intensity correlates with the frequency shift, except in the saturation regime (Fig. 5). We quantify the temperature dependence of the integrated intensity as

$$\Delta I^2 \propto Q^4 \propto |T - T_c|$$

and find that the transition is tricritical in character (for recent reviews of the theory of relationship between phonon intensities and structural phase transitions see Bismayer 1988; Güttler 1990; Salje 1992).

The MC⇔OS transition occurs at ~388 K when the intensity of the 540 cm^{-1} mode goes to zero and new modes at 470 cm^{-1} and 490 cm^{-1} appear. The temperature evolution of the intensity of the 540 cm^{-1} mode (Fig. 6) shows two discontinuities, at ~348 K and at ~373 K. The first discontinuity is probably related to the MX-1⇔PO transition, with the second one to the MC⇔OS transition. The latter transition produces a double peak in the heat capacity curve, at 373 K and 388 K, for a powdered sample (De Dombal and Carpenter 1993) and for single crystals (Cellai et al. 1994), suggesting that two structural events occur during the transformation. The first and the second peaks in the heat capacity data probably correspond to the discontinuity at 373 K in Fig. 6 and the disappearance of the 540 cm^{-1} mode at ~388 K, respectively.

The phase transitions at higher temperatures can be seen in the temperature evolution of the 470 cm^{-1} phonon (Fig. 7). Assuming the usual linear quadratic coupling between the phonon coordinate and the thermodynamic order parameter, linearity in such a diagram is indicative of a second order transition (Salje 1992). Using this mode we find that the phase transition near 686 K

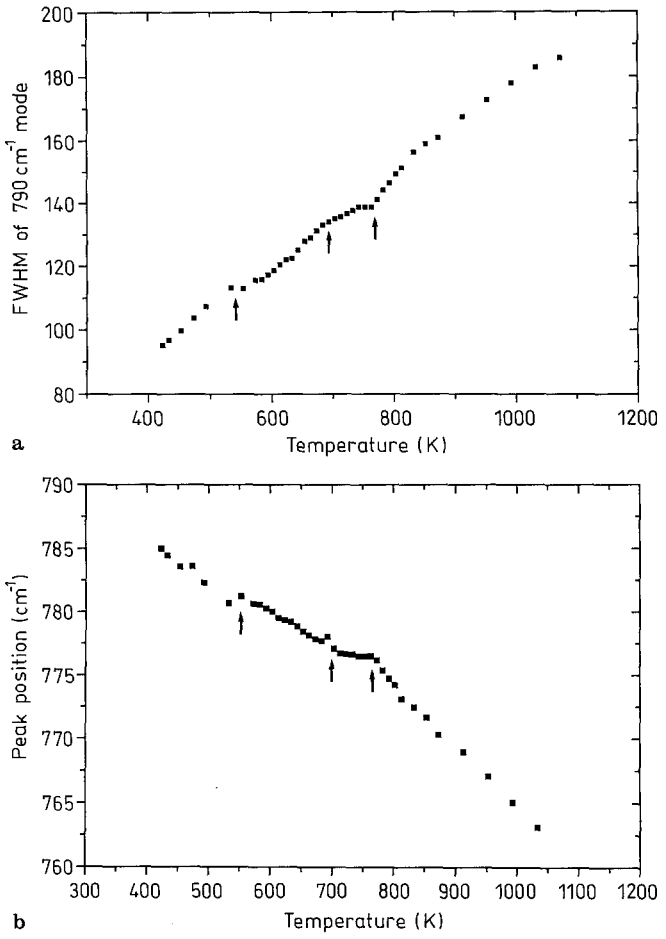

Fig. 8a, b. Temperature dependence of the emission band in the 790 cm^{-1} region for hand-ground Steinbach tridymite. The mode shows transition related changes in mean hard-mode width (**a**) and frequency (**b**) corresponding to phase transitions (Fig. 1) as being near 523 K, 680 K and 748 K

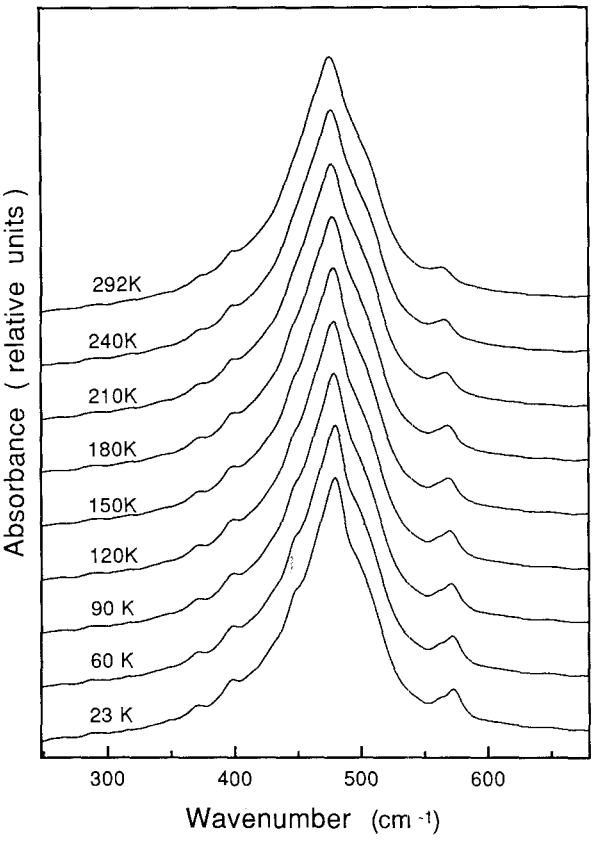

Fig. 9. Infrared absorption spectra for milled powder Steinbach tridymite from room temperature to 23 K. These spectra are very different from those measured for the coarser material (Fig. 2a). The modes are broader and some (e.g. 450 cm^{-1}) disappear when the sample is milled

(LHP⇔HP) is indeed second order, consistent with the calorimetry measurements of Cellai et al. (1994). The stability field of the OC phase takes on a new significance in the light of the IR results. If the OC phase did not occur, it appears that the OS phase would undergo a second order transition to the phase LHP on heating to $T_c = 641$ K. The softening of the OS structure is interrupted by the OC phase field before this transition can actually occur, however. The OC phase can be interpreted as an intermediate structural state uncorrelated with the linear decrease of the intensity of the 470 cm^{-1} mode at lower temperatures, therefore. This intermediate phase is characterised by an increase of the absorbance which remains large in the LHP phase before it finally disappears in the HP phase. The phases most closely related, as shown by this phonon, are (a) LHP and HP, and (b) LHP and OS with real or projected second order phase transitions LHP⇔HP and LHP⇔OS. The OC phase is "parasitic" in the sense that it restabilizes the orthorhombic distortion and overprints the OS⇔LHP transition.

We have desisted from presenting a quantitative analysis of our spectra at temperatures below room temperature because no information is available for the actual structural state of tridymite under these conditions. We note, however, that the temperature evolution of these spectra seem to indicate that tridymite possesses a well defined, almost defect free low temperature structure which may well undergo further phase transitions.

The main difference between the absorption spectra of tridymite and quartz (Salje et al. 1992) is the relatively large line widths of phonon signals between 600 cm^{-1} and 1400 cm^{-1} in tridymite. These modes have been investigated using the emission technique. The temperature evolution of the line width (FWHM) and the peak position of the 790 cm^{-1} phonon are shown in Fig. 8a and Fig. 8b respectively. Several anomalies can be seen in the data in Fig. 8. They correspond to the phase transitions shown in Fig. 1 as being near 748 K, 680 K and 523 K.

The sensitivity of tridymite to prior treatment is found not only at an average structure level, as observed by X-ray diffraction, but also on a much more local level as seen by hard mode spectroscopy. In Fig. 9 spectra of a sample which had been milled for 20 minutes to a fine powder using a ball mill are shown. These spectra were measured under exactly the same conditions as the coarser material shown in Fig. 2c. A comparison of the two sequences reveals dramatic differences. The bond bending modes are broader, showing either structural

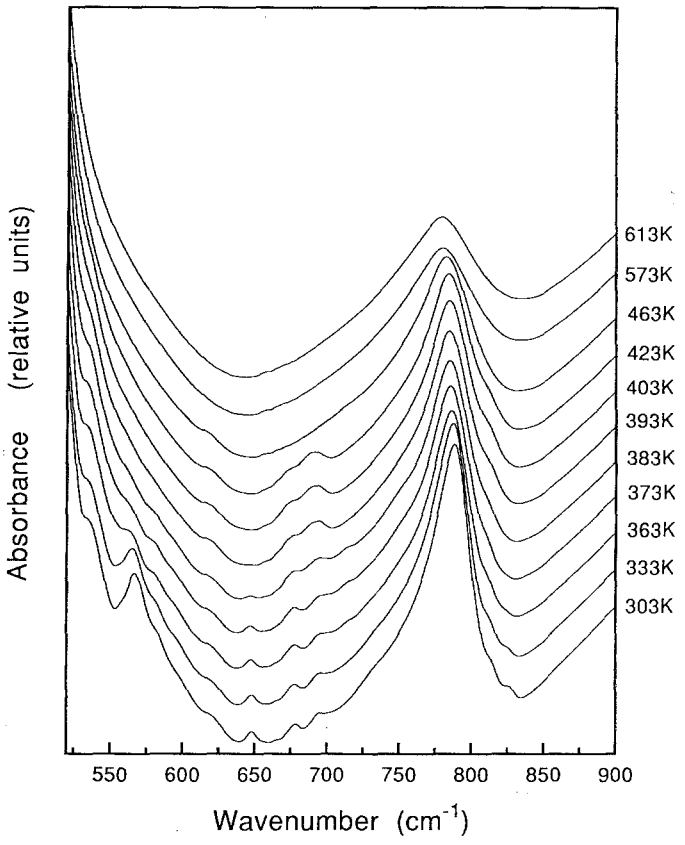

Fig. 10. Infrared absorption spectra for hand-ground synthetic tridymite. These spectra have additional modes in the region 600–750 cm^{-1}, when they are compared with those of hand-ground meteoritic tridymite (Figs. 2 and 3)

imperfections or additional symmetry changes in the fine grained material. Specific phonon signals (e.g. at 540 cm^{-1}) disappear completely when the sample is milled, others became broader (e.g. at 450 cm^{-1}), others stronger (e.g. at 360 cm^{-1}), and others weaker (e.g. at 350 cm^{-1}). These changes can not be understood in terms of simple strain deformation but correspond to topological changes of the crystal structure. Further analytical work is needed to characterise the changes more fully. In view of the systematic changes in the phonon spectra, we expect the structural changes not to be due simply to a random "squeeze" of the framework but to involve systematic changes of the bond angles between rather rigid SiO_4 tetrahedra.

Synthetic Tridymite

The spectra of hand-ground synthetic tridymite were measured separately in the spectral region between 500 cm^{-1} and 900 cm^{-1} for temperatures above 303 K (Fig. 10). These spectra (Fig. 10) are similar to those reported by Görlich et al. (1983) for their synthetic tridymite. The temperature evolution of the spectra is marked by abrupt changes and the disappearance of phonon signals upon heating. The phonon signal near 570 cm^{-1} reduces continuously and disappears before 383 K. This mode is clearly related to the MX-1⇔PO transition.

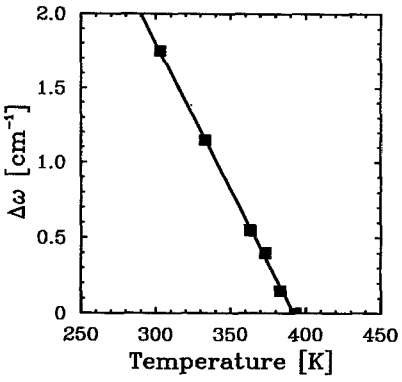

Fig. 11. Temperature dependence of the frequency shift of the 648 cm^{-1} mode for synthetic hand-ground tridymite. The *straight line* is a least-squares fit ($a = -1.9565\ 10^{-2}$ and $b = 7.6710$ for the slope and the intercept respectively) suggesting a second order transition at 388 K

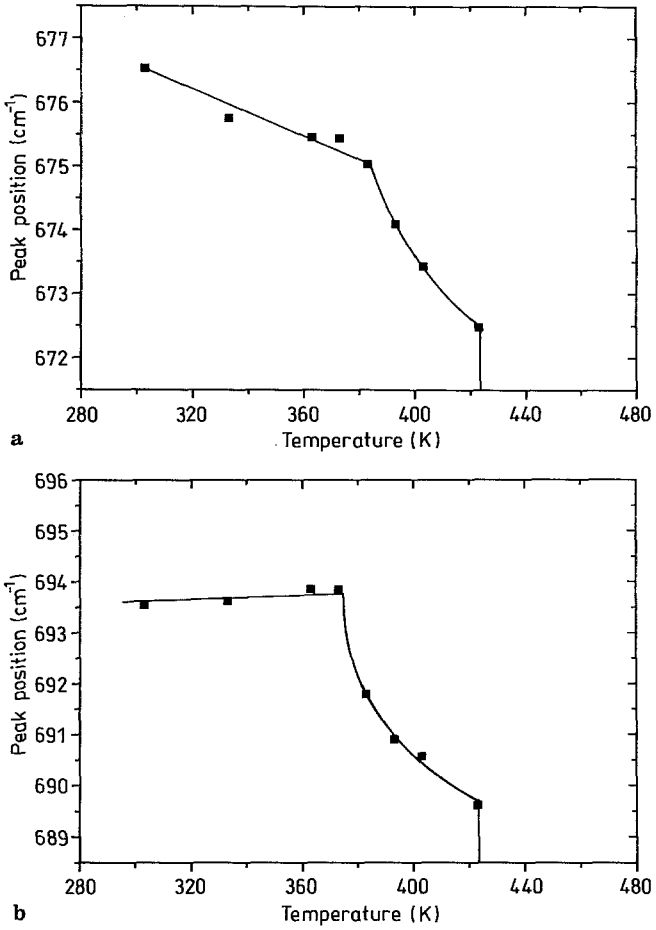

Fig. 12a, b. Temperature dependence of the frequency of the 676 cm^{-1} (**a**) and 690 cm^{-1} (**b**) modes for synthetic hand-ground tridymite. The two anomalies near 388 K and 423 K correspond to the MC⇔OP and OP⇔OS phase transitions. *Solid lines* are a guide for the eyes to emphasize the breaks in slope

The phase transition MC⇔OP at 385 K is correlated with the disappearance of the two phonon signals in the MC phase at 648 cm^{-1} and 540 cm^{-1}. The temperature dependence of the frequency shift ($\Delta\omega = \omega_{383} - \omega_t$) of the 648 cm^{-1} mode is shown in Fig. 11. $\Delta\omega$ decreases linearly with increasing temperature which indicates that

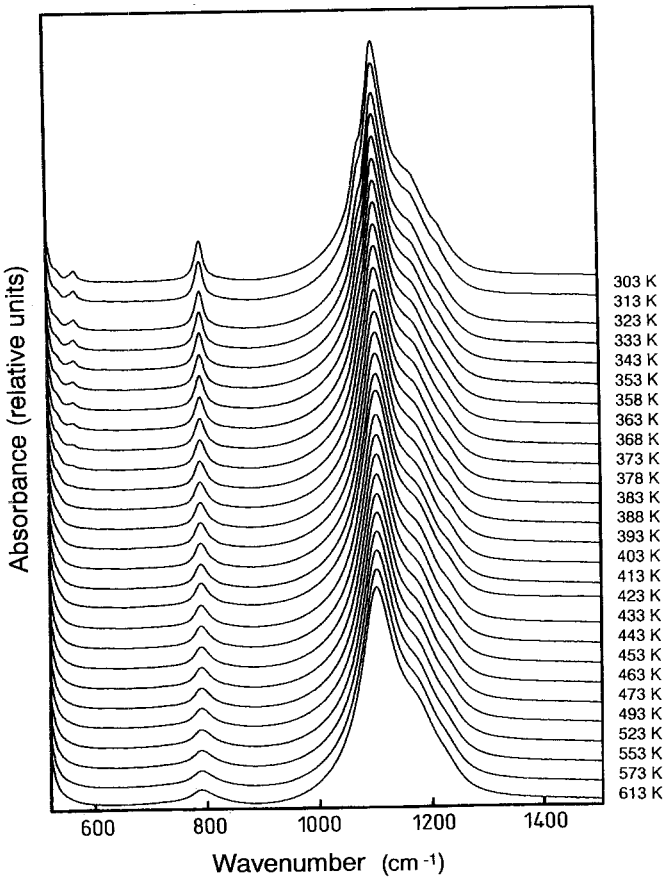

Fig. 13. Infrared absorption spectra of milled powder of synthetic tridymite from room temperature to 613 K. These spectra are different from those of the hand-ground sample due to the absences of modes in the region 600–750 cm^{-1}

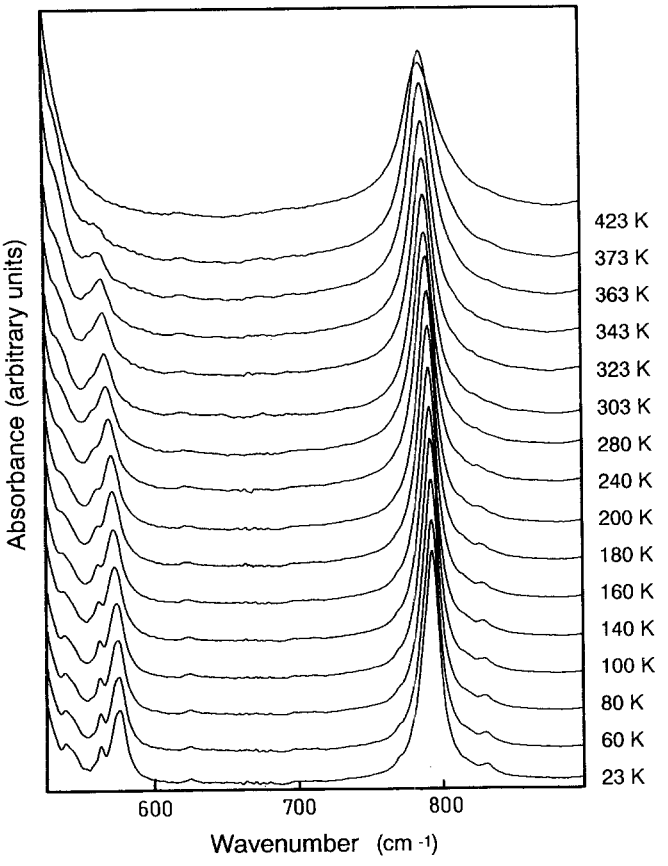

Fig. 14. Infrared absorption spectra of milled powder of synthetic tridymite from room temperature to 23 K. The spectra above room temperature were collected in the heating run and have been considered for comparison

the transition is second order in character, in contrast with the equivalent transition in the meteoritic sample which is first order. The OS phase is reached at ~423 K during heating, and the OP⇔OS transition is seen in the temperature evolution of the modes near 676 cm^{-1} and 690 cm^{-1} (Fig. 12). These two modes also couple with the MC⇔OP phase transition near 385 K. The frequency and integrated intensity of the 690 cm^{-1} signal is almost independent of temperature in the MC phase, i.e. the structural changes do not alter this vibration. The MC⇔OP transition then appears as a change in slope of the temperature dependence of the frequency, without any abrupt change in the absolute values. Thus the transition is seen by this phonon as a continuous process. At the OP⇔OS transition temperature there is a jump in the absolute values of the frequencies of both the modes shown in Fig. 12 and this transition is first order in character, therefore.

Similarly to the meteoritic tridymite, milling of synthetic tridymite leads to dramatic changes of the IR spectra, indicating substantial structural changes (Fig. 13 and Fig. 14). The spectra are very different from the hand ground sample due to the absence of modes in the region 600–700 cm^{-1}. However, on heating, a sequence of phase transitions similar to the hand-ground sample can be identified from the temperature dependence of the frequency of the 790 cm^{-1} band, as shown in Fig. 15 where four discontinuities in the slope at ~350 K, ~385 K, ~423 K and ~490 K are visible. These discontinuities may indicate the MX-1⇔PO, MC⇔OP, OP⇔OS, and OS⇔OC transitions, respectively.

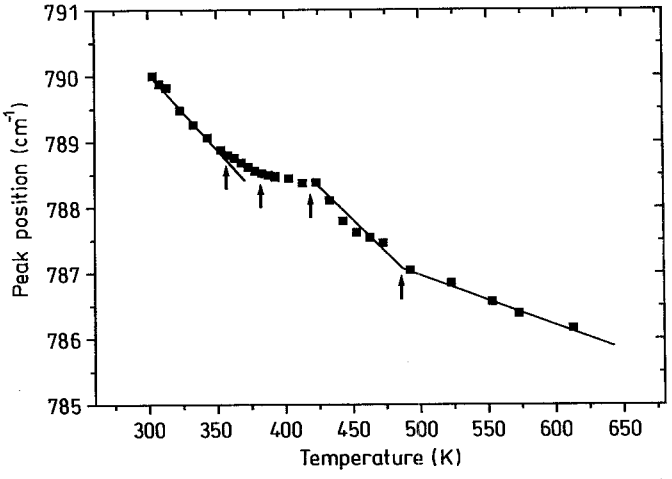

Fig. 15. Temperature dependence of the frequency of the 790 cm^{-1} mode for milled synthetic tridymite showing four anomalies, probably corresponding to the MX-1⇔PO, MC⇔OP, OP⇔OS and OS⇔OC phase transitions

Discussion of Steinbach Tridymite

IR experiments have monitored the changes in symmetry which occur in Steinbach tridymite during heating. These changes can be correlated with anomalies in the heat capacity curve and with changes in the temperature dependence of a reflection violating the *c* glide observed in the previous paper (Cellai et al. 1994).

LHP⇔HP

At high temperatures the infrared spectra of meteoritic tridymite have three main bands at 480 cm^{-1}, 780 cm^{-1} and 1100 cm^{-1} and are similar to the infrared spectra of quartz, where the bands near 1100 cm^{-1} are roughly assigned to Si−O stretching motions, the band near 790 cm^{-1} to Si−O−Si bending and the bands at 500 cm^{-1} to O−S−O bending (Etchepare et al. 1978). The LHP⇔HP transition is characterized by the disappearance of the 470 cm^{-1} mode at 685 K, reducing the total number of peaks from 8 to 7 in the HP phase, as expected from factor group analysis. All seven symmetry allowed modes of the HP phase were found: 460 cm^{-1}, 490 cm^{-1}, 790 cm^{-1}, 960 cm^{-1}, 1050 cm^{-1}, 1150 cm^{-1} and 1200 cm^{-1}.

The disappearance of the 470 cm^{-1} mode (Fig. 7) coincides both with the Cp anomaly of second order character in the specific heat and with a broadening of the reflections violating the *c* glide (*hhl* with *l* odd). This phase transition has been attributed to the beginning of flipping movements of oxygen atoms by Cellai et al. (1994). In the temperature range 620–685 K the symmetry of tridymite is hexagonal and the oxygen atoms occupy statistically all the six positions and around the circumference of the circle perpendicular to the Si-O-Si axis. They may overcome the potential barrier located between any two neighbouring split atom positions but they do not flip over the central barrier, and the average structure is $P6_322$. At 680 K the oxygens start to overcome the central barrier, the crystals acquire the centre of symmetry, and the space group becomes $P6_3/mmc$. Because the flipping does not occur frequently at these temperature, microdomains of the LHP phase are still present up to 748 K, and can be detected at the X-ray scale because broad and weak reflections *hhl* with *l* odd are present until 748 K. At 748 K the disappearence of the reflection correlates with changes in the *c* parameter and with the disappearance of the tail in the excess specific heat above $T_c = 680$ K (Cellai et al. 1994). In the infrared spectra the 748 K anomaly can be seen as a change of the temperature dependence of the 790 cm^{-1} mode. This bending mode has a large frequency shift over the full temperature range. A change in the slope occurs at 693 K and 760 K at which temperatures, approximately, Cellai et al. (1994) noted the Cp anomaly and the appearence of the spontaneous strain e_{33} respectively.

On the length scale of X-ray diffraction the symmetry of tridymite is $P6_3/mmc$ above 748 K (i.e. when the *hhl* with *l* odd reflections have no intensity), although a broadening of these reflections is observed at 680 K indicating that microdomains of HP phase are already present. At an IR scale tridymite has space group $P6_3/mmc$ (i.e. only seven modes) at around 680 K because this technique operates at a shorter length scale than X-ray diffraction and detects shorter range correlations.

OC⇔LHP

The transition OC⇔LHP is not instantly apparent upon inspection of the spectra: the change in symmetry does not obviously produce the peak splitting expected from the group analysis. The 25 modes of the OC phase (Table 2) are probably too near each other to be distinguished. Closer examination of the temperature dependence of the 470 cm^{-1} band provides some evidence of this phase (Fig. 7). This transition does not produce a change in the *c* dimension and cell volume or a Cp anomaly, and can be identified on an X-ray scale only by the splitting of the non 00*l* (*l* odd) reflections in the X-ray traces. According to the X-ray powder data of De Dombal and Carpenter (1993), the orthorhombic⇔hexagonal transition appears to be continuous, occurring at 623 K when the spontaneous strain component e_{11} goes to zero.

OS⇔OC

The transition can be identified at ~513 K (Fig. 7) by the change in the intensity of the 470 cm^{-1} band. This transition also gives a step in the heat capacity curve and a change in the slope of the reflection violating the *c* glide. The Cp anomalies within the stability field of the OS phase, perhaps due to some changes of the incommensurate modulation, are not correlated with any significant features in our IR measurements.

MC⇔OS

The MC⇔OS transition is clearly shown by the disappearance of the 540 cm^{-1} mode at ~388 K (Fig. 6). The transition produces a double peak in the heat capacity curve for a powdered sample (De Dombal and Carpenter 1993) and for single crystals (Cellai et al. 1994). The double peak in the heat capacity curve suggests two structural events during the transformation. The two events could be related to two types of domains, each of which inverts to the OS phase at different temperatures or they may be related to two changes in symmetry. From our IR measurements we do have evidence for two different structural events in the small temperature range between 373 K and 388 K. The first and the second peak in the heat capacity data correlate with the discontinuity in the slope of the temperature dependence of the intensity of the 540 cm^{-1} mode at ~373 K (Fig. 6) and with the disappearance of this mode at ~385 K, respectively. The transition MC⇔OS or MC⇔OP apparently proceeds via an intermediate phase which is stable in a small tem-

perature interval of ~12 K. This result is compatible with the subgroup-supergroup relationships of the phases involved. The space group of MC is not a subgroup of the OP phase (OP is a subgroup of the HP phase). The minimal supergroup common to the MC and OP phases in *Cmcm*, and this could be the symmetry of the phase stable between MC and OP.

Low Temperature Transition

The present IR experiments showed a transition at ~348 K which has not been reported in the previous X-ray and calorimetry study of single crystals of Steinbach tridymite (Cellai et al. 1994). The presence of this phase transition is consistent with the occurence of MX-1 grains in the Steinbach sample. MX-1 is known to form during grinding of large crystals of MC tridymite, and the transformation can be complete or partial (Hoffmann et al. 1983). In the TEM study of synthetic and meteoritic tridymite, Carpenter and Wennemer (1985) identified grains with MC structure and grains with MX-1 structure in crushed Steinbach tridymite. Preparation of crystals for the IR study must inevitably also have led to the formation of some of the MX-1 phase. According to the single X-ray diffraction study of Hoffmann et al. (1983), MX-1 transforms into the pseudo-orthorhombic PO phase in the temperature range 308 K to 353 K, and this is presumably the transformation indicated by the IR data. It is equivalent to the S1⇔S2 transition as seen in the powder X-ray diffraction study by Sato (1964). This transition is probably not completely reversible because, on cooling, the formation of MX-1 phase starts at 333 K, and at 273 K only 60% of PO phase is retransformed to MX-1 (Hoffmann et al. 1983). According to Nukui and Nakazawa (1980) the PO phase has the same sequence of phase transitions on further heating as the MC structure.

Comparison of Steinbach and Synthetic Tridymite

At room temperature the synthetic and meteoritic samples have different spectra in the region 600–750 cm^{-1}. According to Dowty (1987), who calculated infrared spectra for cristobalite and tridymite, modes in the region 600–750 cm^{-1} are characterized by intertetrahedral rotations. When all the intertetrahedral rotations are in the same sense as in cristobalite (all tetrahedra are in the trans configuration) there are additional modes in the region 600–750 cm^{-1}, while, when two-thirds of the tetrahedra are in the trans configuration (those within the sheets) and one-third is in the cis configuration (those in the layer) as in tridymite, the spectra do not have bands in the region 600–750 cm^{-1}. Perhaps the synthetic sample contains mistakes in the intertetrahedral rotation leading to a different average of the ratio of cis and trans configurations with respect to those of tridymite. This may explain the presence of bands in the region 600–750 cm^{-1} in the synthetic sample, which are characteristic of a non tridymite arrangement. Moreover, in synthetic tridymite, the mode at 620 cm^{-1}, which is characteristic of low cristobalite, can be attributed to the presence of cristobalite structurally mixed with tridymite.

It should be emphasised that at room temperature a mixture of phases exist in fine grained Steinbach and synthetic tridymite. The presence of the MX-1 phase is revealed by the MX-1⇔PO transition identified in both Steinbach and synthetic tridymite.

Meteoritic and synthetic samples have one transformation temperature in common. The transition at ~385 K corresponds to the MC⇔OS transition for the meteoritic sample and to the MC⇔OP transition for the synthetic sample. The synthetic sample has an additional phase transition ~423 K from OP to OS. This transition is indicated by the disappearance of the modes at 670 cm^{-1} and 690 cm^{-1} in spectra from the hand-ground sample. Spectra from the synthetic milled sample do not have these two modes, but the transition at ~423 K is identified by the temperature dependence of the 790 cm^{-1} band.

Acknowledgements. The authors would like to thank the British Natural History Museum for the sample of Steinbach tridymite. D. Cellai acknowledges receipt of a EEC (Human Capital an Mobility) fellowships and thanks the Ministero dell'Università e della Ricera Scientifica e Tecnologica in Italy (MURST 40%). R.J. Kirkpatrick acknowledges receipt of a NSF grant (EAR 93-15695).

References

Bismayer U (1988) New developments in Raman spectroscopy on structural phase transitions. In: Salje EKH (ed) Physical properties and thermodynamic behaviour of minerals. NATO ASI C: 225, Reidel, Dordrecht, pp 143–183

Carpenter MA, Wennemer M (1985) Characterization of synthetic tridymites by transmission electron microscope. Am Mineral 70:517–528

Cellai D, Carpenter MA, Wruck B, Salje EKH (1994) Characterization of high temperature phase transitions in single crystals of Steinbach tridymite. Am Mineral 79:606–614

De Dombal RF, Carpenter MA (1993) High-temperature phase transitions in Steinbach tridymite. Eur J Mineral 5:607–622

Dollase WA (1967) The crystal structure at 220 °C orthorhombic high tridymite from the Steinbach meteorite. Acta Crystallogr 23:617–623

Dollase WA, Baur WH (1976) The superstructure of meteoritic low tridymite solved by computer simulation. Am Mineral 61:971–978

Dowty E (1987) Vibrational interactions of tetrahedra in silicate glasses and crystal: II. Calculations on melilites, pyroxenes, silica polymorphs and feldspars. Phys Chem Minerals 14:122–138

Etchepare J, Merian M, Kaplan P (1978) Vibrational normal modes of SiO2 II. Cristobalite and tridymite. J Chem Phys 68:1531–1537

Gibbs RE (1927) The polymorphism of silicon dioxide and the structure of tridymite. Proc Soc Lond A 13:351–368

Görlich E, Blaszczak K, Handke M (1983) Infrared spectra of silica polymorph. Mineral Pol 14:3–18

Graetsch H, Flörke OW (1991) X-ray powder diffraction patterns and phase relationship of tridymite modifications. Z Kristallogr 195:31–48

Güttler B (1990) Elastic phase transitions in minerals and hard mode infrared spectroscopy – some examples. In: Salje EKH (ed) Phase transitions in ferroelastic and co-elastic crystals. Cambridge University Press, Cambridge, England, pp 230–252

Hoffmann W (1967) Gitterkonstanten und Raumgruppe von Tridymite bei 20 °C. Naturwiss. 54:114

Hoffmann W, Kockmeyer M, Löns J, Vach Chr (1983) The transformation of monoclinic low-tridymite MC to a phase with an incommensurate superstructure. Fortschr Mineral 61 1:96–98

Kato K, Nukui A (1976) Die Kristallstruktur des monoklinen Tief-Tridymits. Acta Cryst B 32:2486–2491

Kihara K (1977) An orthorhombic superstructure of tridymite existing between about 105 and 180 °C. Z Kristallogr 146:185–203

Kihara K (1978) Thermal change in unit-cell dimensions and a hexagonal structure of tridymite. Z Kristallogr 148:237–253

Kihara K, Matsumuto T, Imamura M (1986) High-order thermal motion tensor analyses of tridymite. Z Kristallogr 177:39–52

Konnert J, Appleman D (1978) The crystal structure of low tridymite. Acta Cryst B 84:391–403

Löns J, Hoffmann W (1987) Zur Kristallstruktur der inkommensurablen Raumtemperaturphase des Tridymits. Z Kristallogr 178:141–143

Nukui A, Nakazawa H (1980) Polymorphism in tridymite. J Mineral Soc Japan, Special Vol 2:364–386

Nukui A, Nakazawa H, Akao M (1978) Thermal changes in monoclinic tridymite. Am Mineral 63:1252–1259

Salje EKH (1992) Hard Mode Spectroscopy: experimental studies of structural phase transitions. Phase Transitions 37:83–110

Salje EKH, Ridgwell A, Güttler, Wruck B, Dove MT, Dolino G (1992) On the displacive character of the phase transition in quartz: a hard-mode spectroscopy study. J Phys Cond Mat 4:571–577

Sato M (1964) X-ray study of tridymite. III – Unit cell dimensions and phase transition of tridymite. Mineral J 4:215–225

Smelik EA, Reeber RR (1990) A study of thermal behaviour of terrestrial tridymite by continuous X-ray diffraction. Phys Chem Minerals 17:197–206

Xiao Y, Kirkpatrick RJ, Kim YJ (1993) Structural phase transitions of tridymite: a ^{29}Si MAS NMR investigation. Am Mineral 78:241–244